

High- Q silica microdisk optical resonators with large wedge angles on a silicon chip

Guanyu Li,¹ Pei Liu,¹ Xiaoshun Jiang,^{1,3,*} Chao Yang,¹ Jiyang Ma,¹ Hongya Wu,¹ and Min Xiao^{1,2,4}

¹National Laboratory of Solid State Microstructures, College of Engineering and Applied Sciences, Nanjing University, Nanjing 210093, China

²Department of Physics, University of Arkansas, Fayetteville, Arkansas 72701, USA

³State Key Laboratory of Modern Optical Instrumentation, Zhejiang University, Hangzhou 310027, China

⁴e-mail: mxiao@uark.edu

*Corresponding author: jxs@nju.edu.cn

Received July 17, 2015; accepted August 18, 2015;

posted August 20, 2015 (Doc. ID 245803); published September 18, 2015

We experimentally demonstrate high optical quality factor silica microdisk resonators on a silicon chip with large wedge angles by reactive ion etching. For 2- μm -thick microresonators, we have achieved wedge angles of 59°, 63°, 70°, and 79° with optical quality factors of 2.4×10^7 , 8.1×10^6 , 5.9×10^6 , and 7.4×10^6 , respectively, from ~ 80 μm -diameter microresonators in the 1550 nm wavelength band. Also, for 1- μm -thick microresonators, we have obtained an optical quality factor of 7.3×10^6 with a wedge angle of 74°. © 2015 Chinese Laser Press

OCIS codes: (140.4780) Optical resonators; (140.3948) Microcavity devices.

<http://dx.doi.org/10.1364/PRJ.3.000279>

1. INTRODUCTION

Whispering gallery mode (WGM) optical microresonators, owing to their high quality factors and small mode volumes, have been widely used in cavity quantum electrodynamics, optical communication, nonlinear optics, chemical/biological sensing, and cavity optomechanics [1,2]. Recently, coupled optical microresonators have attracted more and more attention for their potential applications in coupled-resonator optical waveguides [3,4], analogues to electromagnetically induced transparency [5–7], quantum information processing [8,9], phonon lasers [10], parity-time-symmetric optics [11,12], etc.

So far, chip-based high- Q optical microresonators have been realized using various kinds of materials such as silicon [13,14], silicon nitride [15], silica [16–19], III–V semiconductor [20,21], polymer [22,23], and diamond [24]. Among them, silica optical microresonators, in the forms of toroid [16], sphere [17], and disk [18,19], exhibit ultrahigh optical quality factors on chip due to their ultralow material absorption and extremely smooth surfaces. For the silica microrotoroid [16] and microsphere [17] cavities, their quality factors are obtained by reducing the surface roughness down to atomic scale with the help of CO₂ laser reflow. However, this process significantly shrinks the diameters of the microcavities, which limits their applications in device integration and makes it challenging to fabricate two or more microcavities close to each other on the same silicon chip. Recently, a wedge-shaped silica disk resonator (7.5 mm diameter) with a wedge angle smaller than 30° has achieved the record optical quality factor of 8.75×10^8 on chip [19]. However, to boost the optical quality factor of this structure, the silica disk is over etched using buffered HF, which makes the size of the disk smaller than the original pattern on the photomask [18,19]. Also, the small-angle wedge structure pushes the optical WGMs away from

the disk perimeter [18,19], which further limits certain device applications in coupled microresonators.

Here, we fabricate a class of high optical quality factor silica microdisk resonators with large wedge angles using the reactive ion etching process. In previous works, dry-etched silica microdisk resonators including single-layer [25,26] and double-layer [27,28] structures have been demonstrated with quality factors of $\sim 5 \times 10^5$ for coupled microresonators [25,26] and with a quality factor of 1.75×10^6 for gradient-force-actuated cavity optomechanics [27,28]. Moreover, these microdisk resonators were fabricated using metal or e-beam resist as a mask for reactive ion etching, which limited the Q -factor or the thickness of the microresonators. In this work, we demonstrate dry-etched silica microdisk resonators on a silicon chip with large wedge angles due to the anisotropic nature of dry etching using photoresist as an etch mask. We have obtained silica microdisk resonators with thickness as large as 2 μm and a record Q -factor of 2.4×10^7 for dry-etched silica microdisk cavities on chip at the wavelength of ~ 1550 nm.

2. DEVICE FABRICATION AND MEASURED RESULTS

As shown in Fig. 1, the fabrication process for the silica microdisk resonators mainly contains four steps. First, a NSR-1755i7B stepper is used to pattern the photoresist (AZ 6130) on a thermally grown silicon oxide film with a thickness of 1 or 2 μm . After exposure, a post-exposure bake is performed to reduce the sidewall roughness of the photoresist pattern. Then, the reactive ion etching with SF₆/CHF₃/He chemistry is employed to transfer the pattern of the photoresist onto the silicon oxide layer. The residual photoresist after the reactive ion etching is removed using the photoresist remover (AZ remover 700) followed by H₂SO₄/H₂O₂ solution. Finally, the silica microdisk is undercut by the

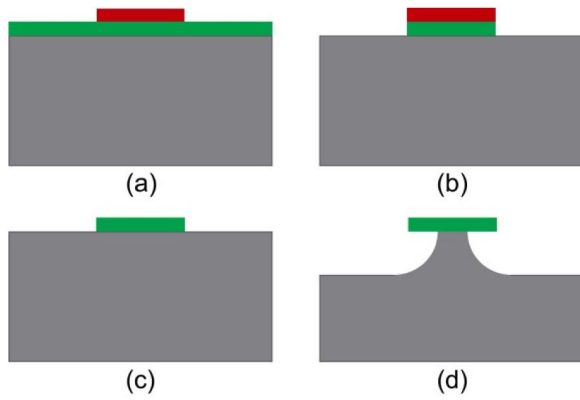


Fig. 1. Fabrication process of the silica microdisk resonator. (a) Photolithography to pattern the photoresist onto a silicon oxide layer. (b) Reactive ion etching to transfer the pattern of the photoresist into the silicon oxide layer. (c) Remove the residual photoresist using photoresist remover and $\text{H}_2\text{SO}_4/\text{H}_2\text{O}_2$ solution. (d) Undercut the silica microdisk resonator using XeF_2 dry etching to form a silicon pillar.

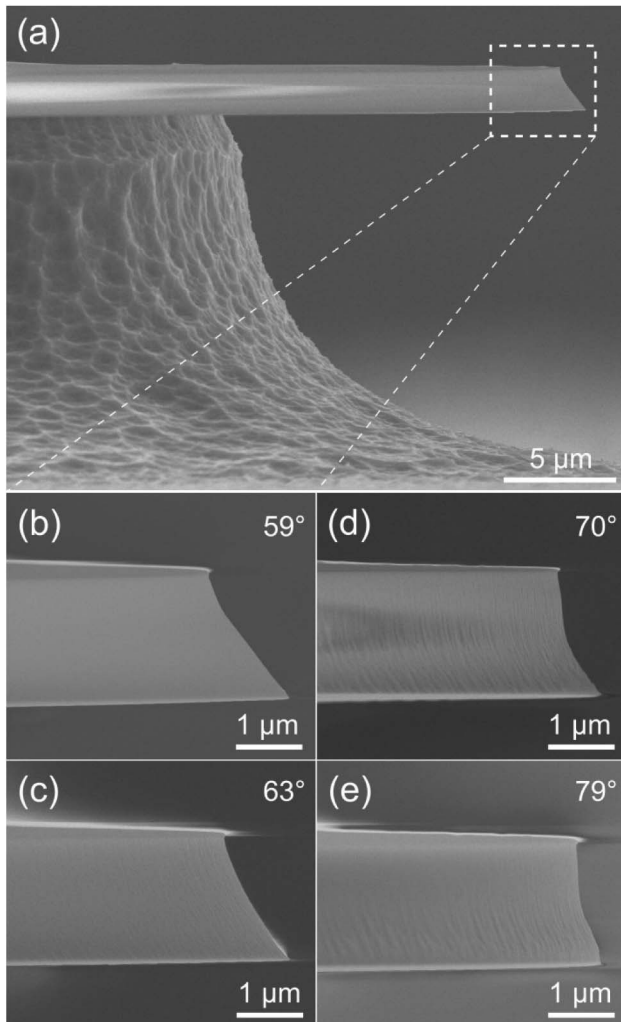


Fig. 2. (a) Side-view SEM image of a silica microdisk resonator with a wedge angle of 59° . (b)–(e) Close-view SEM images of the silica microdisk resonators with wedge angles of 59° , 63° , 70° , and 79° , respectively. The diameter and the thickness of the microdisk resonators are 80 and 2 μm , respectively.

XeF_2 dry etching to form a silicon pillar. Figures 2(a)–2(e) show the typical scanning electron microscope (SEM) images of the fabricated silica microdisk resonators with a thickness of 2 μm . By changing the radio frequency power during the fabrication process, we have obtained silica microdisk resonators with different wedge angles of 59° , 63° , 70° , and 79° , respectively [Figs. 2(b)–2(e)], which are much larger than those of the previously demonstrated silica microresonators fabricated using the buffered HF wet etching process [18,19]. The diameters of the silica microdisks are around 80 μm , which is very close to the size of the patterned photoresist mask.

In order to characterize the fabricated silica microdisk resonator, a tapered optical fiber is used to excite the WGMs of the microresonator via the evanescent wave [29]. A tunable external cavity semiconductor laser (New Focus, model TLB-6328) with a linewidth of less than 300 kHz is coupled into the fiber taper to measure the transmission spectrum of the microresonator by scanning the wavelength of the laser. During the experiment, the measured resonant linewidths of the cavity modes are calibrated by a fiber Mach-Zehnder interferometer, and the silica microdisk resonator is kept in a nitrogen-purged enclosure to prevent unwanted water and particle contaminations.

Figure 3(a) shows the measured transmission spectrum of a fundamental TE-like mode from the 59° -wedge-angle silica microdisk resonator with a thickness of 2 μm and a diameter

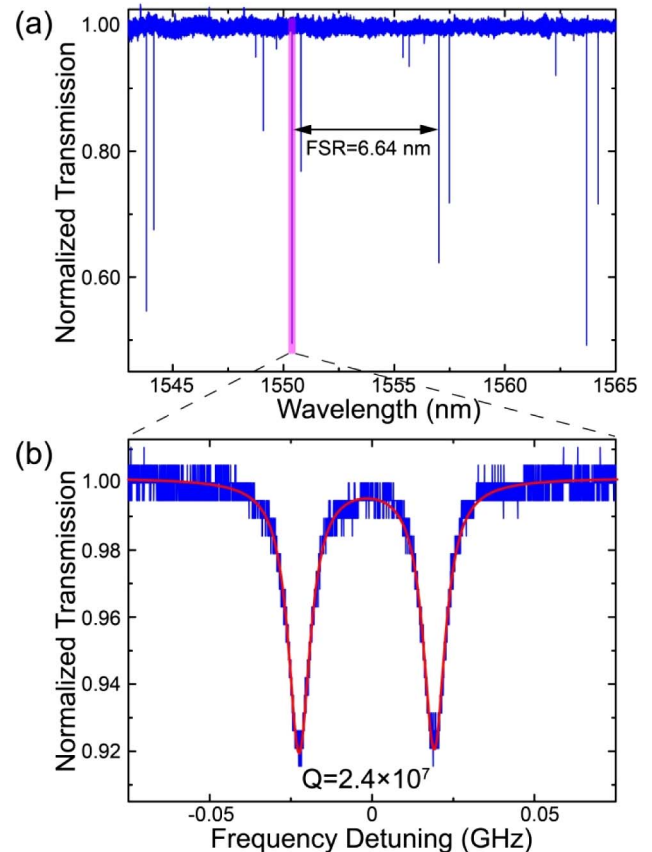


Fig. 3. (a) Normalized transmission spectrum of a fundamental TE-like mode from a 2- μm -thick silica microdisk resonator with the wedge angle of 59° . (b) Detailed scan spectrum of the high-Q cavity mode at the wavelength of ~ 1550.4 nm.

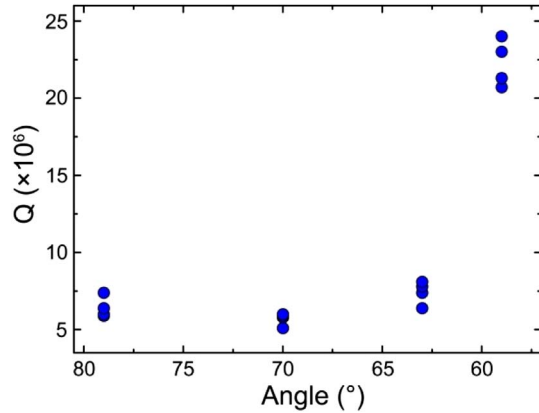


Fig. 4. Experimentally realized quality factors of the silica microdisk resonators with different wedge angles. The diameter and the thickness of the microdisk resonators are kept to 80 and 2 μm , respectively.

of $\sim 80 \mu\text{m}$. The measured free spectral range (FSR) is 6.64 nm, in good agreement with the value calculated from the diameter of the silica microdisk. Figure 3(b) presents the detailed transmission spectrum of this fundamental mode at the wavelength of $\sim 1550.4 \text{ nm}$. The doublet feature in the transmission spectrum is due to the mode splitting caused by the mode coupling between the clockwise and counterclockwise propagation modes [30]. The measured intrinsic quality factor for this microdisk resonator is 2.4×10^7 , corresponding to a finesse of $\sim 1.0 \times 10^5$. This optical quality factor of the dry-etched microdisk resonator is ~ 48 times higher than the previously reported single-layer silica microdisk resonators [25,26], ~ 14 times larger than the double-layer silica microdisk resonator [27,28], and even closer to the wet-etched silica microdisk resonators with similar diameter and thickness [18,19]. Figure 4 shows the intrinsic quality factors of the experimentally realized silica microdisk resonators with different wedge angles of 59° , 63° , 70° , and 79° . The best quality factors for the 63° , 70° , and 79° microresonators are 8.1×10^6 , 5.9×10^6 , and 7.4×10^6 , respectively. Here, the difference in the quality factors for different wedge-angle microresonators is mainly determined by the roughness of the sidewall induced during the reactive ion etching, as shown in Fig. 2. In addition, in order to get a smaller mode volume for the microresonator, we have also fabricated 1- μm -thick silica microdisk resonators with a wedge angle of 74° and obtained the optical Q -factor to be as large as 7.3×10^6 . The optical quality factors of the dry-etched silica microdisk resonators might be further improved by optimizing the fabrication processes, such as the photolithography and reactive ion etching, as well as fabricating disk resonators with larger diameter and thicker silicon oxide layer [19].

3. DISCUSSION

As the dispersion is very important in many nonlinear processes, e.g., parametric oscillation [31], it is worth mentioning that the geometric dispersion and hence the total dispersion can be efficiently controlled by changing the wedge angles. Figure 5 shows the simulated group velocity dispersion of the fundamental TE-like mode for the silica microdisk resonators with wedge angles of 30° , 59° , and 79° , from which we can clearly see that the zero dispersion points shift significantly to shorter wavelengths with the increase of the wedge

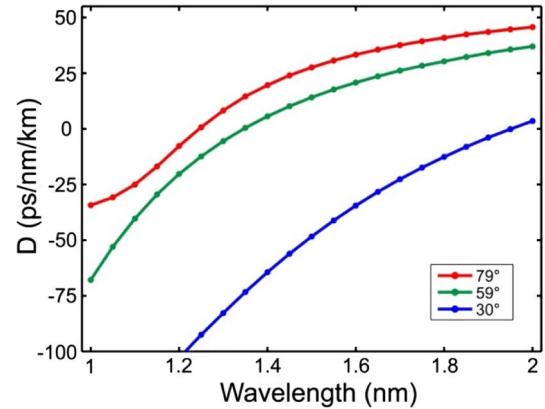


Fig. 5. Simulated group velocity dispersion as a function of wavelength for the fundamental TE-like mode of the silica microdisk resonators with wedge angles of 30° , 59° , and 79° . The diameter and the thickness of the microdisk resonators are kept to 80 and 2 μm , respectively.

angles [32]. Also, the dispersion of the microdisk resonators with larger wedge angles moves to the anomalous dispersion region in the 1550 nm wavelength band, which will be helpful for the generation of Kerr frequency combs [33–35].

4. CONCLUSIONS

In conclusion, dry-etched silica microdisk resonators with different large wedge angles have been demonstrated on a silicon chip. A Q -factor as high as 2.4×10^7 is observed from an 80- μm -diameter microdisk resonator with a thickness of 2 μm and a wedge angle of 59° . This kind of high- Q silica microdisk resonator with a large wedge angle will enable monolithic integration of the microdisk resonators coupled to a waveguide and will be useful in coupled-resonator optical waveguides, nonlinear optics, and cavity optomechanics.

ACKNOWLEDGMENT

The authors thank Xuewei Wu for technical assistance. This work was supported by the National Basic Research Program of China (Nos. 2012CB921804 and 2011CBA00205) and the National Natural Science Foundation of China (Nos. 61435007 and 11321063).

REFERENCES

1. K. J. Vahala, "Optical microcavities," *Nature* **424**, 839–846 (2003).
2. M. Aspelmeyer, T. J. Kippenberg, and F. Marquardt, "Cavity optomechanics," *Rev. Mod. Phys.* **86**, 1391–1452 (2014).
3. A. Yariv, Y. Xu, R. K. Lee, and A. Scherer, "Coupled-resonator optical waveguide: a proposal and analysis," *Opt. Lett.* **24**, 711–713 (1999).
4. F. Morichetti, C. Ferrari, A. Canciamilla, and A. Melloni, "The first decade of coupled resonator optical waveguides: bringing slow light to applications," *Laser Photon. Rev.* **6**, 74–96 (2012).
5. A. Naweed, G. Farca, S. I. Shopova, and A. T. Rosenberger, "Induced transparency and absorption in coupled whispering-gallery microresonators," *Phys. Rev. A* **71**, 043804 (2005).
6. K. Totsuka, N. Kobayashi, and M. Tomita, "Slow light in coupled-resonator-induced transparency," *Phys. Rev. Lett.* **98**, 213904 (2007).
7. C. Zheng, X. Jiang, S. Hua, L. Chang, G. Li, H. Fan, and M. Xiao, "Controllable optical analog to electromagnetically induced transparency in coupled high- Q microtoroid cavities," *Opt. Express* **20**, 18319–18325 (2012).

8. A. Dousse, J. Suffczyński, A. Beveratos, O. Krebs, A. Lemaitre, I. Sagnes, J. Bloch, P. Voisin, and P. Senellart, "Ultrabright source of entangled photon pairs," *Nature* **466**, 217–220 (2010).
9. A. Majumdar, A. Rundquist, M. Bajcsy, V. D. Dasika, S. R. Bank, and J. Vučković, "Design and analysis of photonic crystal coupled cavity arrays for quantum simulation," *Phys. Rev. B* **86**, 195312 (2012).
10. I. S. Grudin, H. Lee, O. Painter, and K. J. Vahala, "Phonon laser action in a tunable two-level system," *Phys. Rev. Lett.* **104**, 083901 (2010).
11. L. Chang, X. Jiang, S. Hua, C. Yang, J. Wen, L. Jiang, G. Li, G. Wang, and M. Xiao, "Parity-time symmetry and variable optical isolation in active-passive-coupled microresonators," *Nat. Photonics* **8**, 524–529 (2014).
12. B. Peng, S. K. Özdemir, F. Lei, F. Monifi, M. Gianfreda, G. L. Long, S. Fan, F. Nori, C. M. Bender, and L. Yang, "Parity-time-symmetric whispering-gallery microcavities," *Nat. Phys.* **10**, 394–398 (2014).
13. M. Borselli, T. J. Johnson, and O. Painter, "Beyond the Rayleigh scattering limit in high-*Q* silicon microdisks: theory and experiment," *Opt. Express* **13**, 1515–1530 (2005).
14. A. Biberman, M. J. Shaw, E. Timurdogan, J. B. Wright, and M. R. Watts, "Ultralow-loss silicon ring resonators," *Opt. Lett.* **37**, 4236–4238 (2012).
15. Q. Li, A. A. Eftekhari, M. Sodagar, Z. Xia, A. H. Atabaki, and A. Adibi, "Vertical integration of high-*Q* silicon nitride microresonators into silicon-on-insulator platform," *Opt. Express* **21**, 18236–18248 (2013).
16. D. K. Armani, T. J. Kippenberg, S. M. Spillane, and K. J. Vahala, "Ultra-high-*Q* toroid microcavity on a chip," *Nature* **421**, 925–928 (2003).
17. J.-B. Jager, V. Calvo, E. Delamadeleine, E. Hadji, P. Noé, T. Ricart, D. Bucci, and A. Morand, "High-*Q* silica microcavities on a chip: from microtoroid to microsphere," *Appl. Phys. Lett.* **99**, 181123 (2011).
18. T. J. Kippenberg, J. Kalkman, A. Polman, and K. J. Vahala, "Demonstration of an erbium-doped microdisk laser on a silicon chip," *Phys. Rev. A* **74**, 051802 (2006).
19. H. Lee, T. Chen, J. Li, K. Yang, S. Jeon, O. Painter, and K. J. Vahala, "Chemically etched ultrahigh-*Q* wedge-resonator on a silicon chip," *Nat. Photonics* **6**, 369–373 (2012).
20. C. P. Michael, K. Srinivasan, T. J. Johnson, O. Painter, K. H. Lee, K. Hennessy, H. Kim, and E. Hu, "Wavelength-and material-dependent absorption in GaAs and AlGaAs microcavities," *Appl. Phys. Lett.* **90**, 051108 (2007).
21. L. Ding, C. Baker, P. Senellart, A. Lemaitre, S. Ducci, G. Leo, and I. Favero, "High frequency GaAs nano-optomechanical disk resonator," *Phys. Rev. Lett.* **105**, 263903 (2010).
22. P. Rabiei, W. H. Steier, C. Zhang, and L. R. Dalton, "Polymer micro-ring filters and modulators," *J. Lightwave Technol.* **20**, 1968–1975 (2002).
23. T. Grossmann, M. Hauser, T. Beck, C. Gohn-Kreuz, M. Karl, H. Kalt, C. Vannahme, and T. Mappes, "High-*Q* conical polymeric microcavities," *Appl. Phys. Lett.* **96**, 013303 (2010).
24. B. J. M. Hausmann, I. Bulu, V. Venkataraman, P. Deotare, and M. Lončar, "Diamond nonlinear photonics," *Nat. Photonics* **8**, 369–374 (2014).
25. C. Schmidt, A. Chipouline, T. Käsebier, E.-B. Kley, A. Tünnermann, T. Pertsch, V. Shuvayev, and L. I. Deych, "Observation of optical coupling in microdisk resonators," *Phys. Rev. A* **80**, 043841 (2009).
26. C. Schmidt, A. Chipouline, T. Käsebier, E.-B. Kley, A. Tünnermann, and T. Pertsch, "Thermal nonlinear effects in hybrid silica/polymer microdisks," *Opt. Lett.* **35**, 3351–3353 (2010).
27. X. Jiang, Q. Lin, J. Rosenberg, K. Vahala, and O. Painter, "High-*Q* double-disk microcavities for cavity optomechanics," *Opt. Express* **17**, 20911–20919 (2009).
28. Q. Lin, J. Rosenberg, X. Jiang, K. J. Vahala, and O. Painter, "Mechanical oscillation and cooling actuated by the optical gradient force," *Phys. Rev. Lett.* **103**, 103601 (2009).
29. M. Cai, O. Painter, and K. J. Vahala, "Observation of critical coupling in a fiber taper to a silica-microsphere whispering-gallery mode system," *Phys. Rev. Lett.* **85**, 74–77 (2000).
30. T. J. Kippenberg, S. M. Spillane, and K. J. Vahala, "Modal coupling in traveling-wave resonators," *Opt. Lett.* **27**, 1669–1671 (2002).
31. T. J. Kippenberg, S. M. Spillane, and K. J. Vahala, "Kerr-nonlinearity optical parametric oscillation in an ultrahigh-*Q* toroid microcavity," *Phys. Rev. Lett.* **93**, 083904 (2004).
32. J. Li, H. Lee, K. Y. Yang, and K. J. Vahala, "Sideband spectroscopy and dispersion measurement in microcavities," *Opt. Express* **20**, 26337–26344 (2012).
33. I. H. Agha, Y. Okawachi, and A. L. Gaeta, "Theoretical and experimental investigation of broadband cascaded four-wave mixing in high-*Q* microspheres," *Opt. Express* **17**, 16209–16215 (2009).
34. Y. K. Chembo and N. Yu, "Modal expansion approach to optical-frequency-comb generation with monolithic whispering-gallery-mode resonators," *Phys. Rev. A* **82**, 033801 (2010).
35. T. Herr, K. Hartinger, J. Riemensberger, C. Y. Wang, E. Gavartin, R. Holzwarth, M. L. Gorodetsky, and T. J. Kippenberg, "Universal formation dynamics and noise of Kerr-frequency combs in microresonators," *Nat. Photonics* **6**, 480–487 (2012).